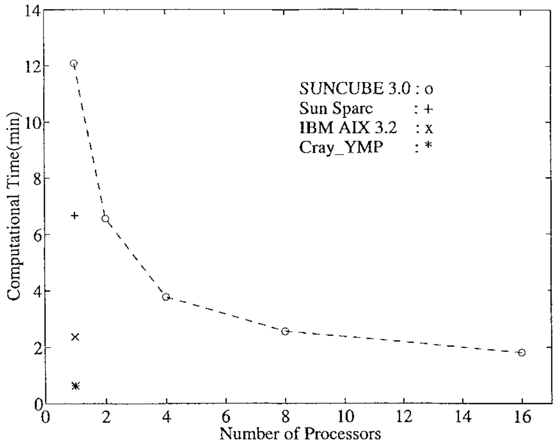

Fig. 3 Computational time vs number of processors for α control.

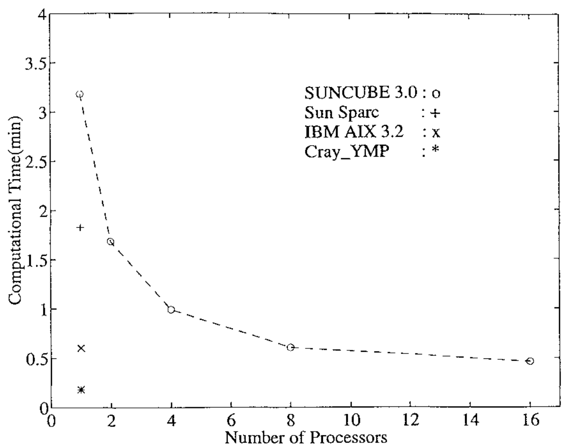

Fig. 4 Computational time vs number of processors for δ control.

are neglected to simplify the problem. The trajectory is divided into 10 subintervals during the first stage and 6 during the second stage. The initial guesses for the costates were the same as used for the previous example.

Figure 1 shows the control variable histories for the two examples. The inequality constraint is active for a short time, during the first stage, when the angle of attack is used as the control variable, as seen from Fig. 1. Figure 2 shows the Hamiltonian histories. The Hamiltonians are zero in the second stage as the final time is free. Figures 3 and 4 show the total computational and communication times (four iterations each) and speedup performance as a function of the number of processors for the two examples. Also included in these figures are the central processing unit (CPU) times for the same code to run on different serial computers. It is observed that the computational time for the second example is much lower than the first due to the elimination of the angle-of-attack dependency of the aerodynamic coefficients.

Conclusions

Implementation of a parallel shooting method on a parallel computer for solving a variety of optimal control and guidance problems has been presented. It is observed that a speedup of nearly 7 to 1 is achieved using 16 processors for the examples considered. Further improvements in performance might be achievable by parallelizing in the state domain.

Acknowledgment

This research is based in part upon work supported by the Texas Higher Education Coordinating Board under grant 999903-264.

References

[1]Bryson, A. E., and Ho, Y. C., *Applied Optimal Control*, Hemisphere, Washington, DC, 1975.

[2]Roberts, S. M., and Shipman, J. S., *Two-Point Boundary Value Problems: Shooting Methods*, American Elsevier, New York, 1972.

[3]Enright, P. J., and Conway, B. A.," Optimal Finite-Thrust Spacecraft Trajectories Using Collocation and Nonlinear Programming," *Journal of Guidance, Dynamics, and Control*, Vol. 14, No. 5, 1991, pp. 981–985.

[4]Keller, H. B., and Nelson, P., "Hypercube Implementations of Parallel Shooting," *Applied Mathematics and Computation*, Vol. 31, 1989, pp. 574–603.

[5]Betts, J. T., and Huffman, W. P., "Trajectory Optimization on a Parallel Processor," *Journal of Guidance, Control, and Dynamics*, Vol. 14, No. 2, 1991, pp. 431–439.

[6]Psiaki, M. L., and Park, K.-H., "Parallel Solver for Trajectory Optimization Search Directions," *Journal of Optimization Theory and Applications*, Vol. 73, No. 3, 1992, pp. 519–546.

[7]Menon, P. K. A., and Lehman, L. L., "A Parallel Quasi-Linearization Algorithm for Air Vehicle Trajectory Optimization," *Journal of Guidance, Control, and Dynamics*, Vol. 9, No. 1, 1986, pp. 119–121.

[8]Miele, A., and Wang, T., "Parallel Computations of Two-Point Boundary-Value Problems via Particular Solutions," *Journal of Optimization Theory and Applications*, Vol. 79, No. 1, 1993, pp. 5–29.

[9]Shaver, D. A., and Hull, D. G., "Advanced Launch System Trajectory Optimization Using Suboptimal Control," AIAA Paper 90-3413-CP, Aug. 1990.

[10]Seywald, H., and Cliff, E. M., "A Feedback Control for the Advanced Launch System," AIAA Paper 91-2619-CP, Aug. 1991.

Maximum Likelihood Estimation of Fractional Brownian Motion and Markov Noise Parameters

Michael E. Ash*
Charles Stark Draper Laboratory, Inc., Cambridge, Massachusetts 02173
and
Matthew E. Skeen†
Cape Canaveral Air Force Station, Florida 32925

I. Introduction and Conclusions

THE parameters in a trend, random walk, exponentially correlated, and white noise Markov approximation to flicker noise [-1 log-log power spectral density (PSD) slope[1–3]] are estimated using maximum likelihood system identification. In addition, parameters for a fractional Brownian motion (fBm)[4,5] model of flicker noise plus trend or white noise are estimated using maximum likelihood gradient iterations, in contrast to previous work using brute force search to estimate a single fBm parameter.[6]

II. Maximum Likelihood Estimation

Let $z^N = [z_1, \ldots, z_N]^T$ be measurements at times $t_1, \ldots, t_N$ with joint probability density $p(z; \alpha)$ dependent on parameters $\alpha = [\alpha_1, \ldots, \alpha_m]^T$. Let $\Delta\alpha_j = \hat{\alpha}_j - \alpha_{j0}$ be adjustments from guesses α_{j0} towards the maximum likelihood estimates $\hat{\alpha}_j$ that minimize the negative log likelihood $\zeta(z^N; \alpha) = -\ln[p(z^N; \alpha)]$. A Taylor series expansion of the gradient of $\zeta(z^N; \alpha)$ yields

$$\sum_{j=1}^{m} A_{ij} \Delta\alpha_j = B_i, \qquad i = 1, \ldots, m \tag{1}$$

$$B_i = -\left.\frac{\partial \zeta(z^N; \alpha)}{\partial \alpha_i}\right|_{\alpha=\alpha_0}, \qquad A_{ij} = \left.\frac{\partial^2 \zeta(z^N; \alpha)}{\partial \alpha_i \partial \alpha_j}\right|_{\alpha=\alpha_0} \tag{2}$$

Received June 15, 1993; revision received March 31, 1994; accepted for publication July 6, 1994.

*Principal Member of Technical Staff. Senior Member AIAA.
†Captain, U.S. Air Force.

The Fisher information approximation replaces A by its expected value $\mathbb{I}$:

$$A_{ij} \approx \mathbb{I}_{ij} \equiv E\left[\frac{\partial^2 \zeta(z^N;\alpha)}{\partial\alpha_i \partial\alpha_j}\right] = E\left[\frac{\partial \zeta(z^N;\alpha)}{\partial\alpha_i}\frac{\partial \zeta(z^N;\alpha)}{\partial\alpha_j}\right] \tag{3}$$

where the covariance of $\hat{\alpha}$ has the Cramer–Rao lower bound[7] $\mathbb{I}^{-1}$.

III. Maximum Likelihood System Identification

Consider the discrete time state space model with vector measurements z:

$$x(t_k) = \Phi(\alpha)x(t_{k-1}) + B(\alpha)u(t_{k-1}) + L(\alpha)\xi(t_{k-1}) \tag{4}$$

$$z(t_k) = H(\alpha)x(t_k) + \theta(t_k) \tag{5}$$

The initial state $x(t_0)$ is a Gaussian random vector with mean $E\{x(t_0)\} = x_0(\alpha)$ and covariance $P_0(\alpha)$. The plant and measurement noise processes are zero mean, discrete, white noises with covariances $E\{\xi(t_j)\xi(t_k)\} = Q(\alpha)\delta_{jk}$ and $E\{\theta(t_j)\theta(t_k)\} = R(\alpha)\delta_{jk}$, respectively.

Given values for the dynamic and stochastic parameters α, running a Kalman filter yields the propagated state $\hat{x}(t_k \mid t_{k-1})$, its covariance $P(t_k \mid t_{k-1})$, the zero mean pre-update residual innovations sequence and its covariance

$$r(t_k) = z(t_k) - H\hat{x}(t_k \mid t_{k-1}) \tag{6}$$

$$S(t_k) = E\{r(t_k)r(t_k)^T\} = HP(t_k \mid t_{k-1})H^T + R(t_k) \tag{7}$$

and the updated state $\hat{x}(t_k)$ and its covariance $P(t_k)$.

The conditional probability density of the measurement $z(t_k)$ at time t_k given measurements and initial condition $z^{k-1} = [z(t_{k-1}), z(t_{k-2}), \ldots, z(t_1), x(t_0)]$ up to time t_{k-1} is

$$p\left[z(t_k) \mid z^{k-1}\right] = (2\pi)^{-\rho/2}\det[S(t_k)]^{-1/2} \times e^{-[r(t_k)^T S(t_k)^{-1} r(t_k)]/2} \tag{8}$$

where ρ is the dimension of the observation vector and $\det(S)$ is the determinant of S. The negative log likelihood of the measurements through time t_N is

$$\zeta(z^N;\alpha) = \sum_{k=1}^{N} \zeta\left[z(t_k) \mid z^{k-1};\alpha\right] + \zeta[x(t_0);\alpha] \tag{9}$$

where by Eq. (8) with n the dimension of the initial state vector $x(t_0)$

$$\zeta\left[z(t_k) \mid z^{k-1};\alpha\right] = \frac{\rho}{2}\ln(2\pi) + \frac{1}{2}\ln\{\det[S(t_k;\alpha)]\} + \frac{1}{2} r(t_k;\alpha)^T S(t_k;\alpha)^{-1} r(t_k;\alpha) \tag{10}$$

$$\zeta[x(t_0);\alpha] = \frac{n}{2}\ln(2\pi) + \frac{1}{2}\ln[\det(P_0)] + \frac{1}{2}[x(t_0) - x_0]^T P_0^{-1}[x(t_0) - x_0] \tag{11}$$

Maximum likelihood system identification[7–11] iteratively uses the equations in Sec. II to estimate α, with the gradient of $\zeta(z^N;\alpha)$ being[10,12]

$$\frac{\partial \zeta(z^N;\alpha)}{\partial\alpha_i} = \sum_{k=1}^{N} \frac{\partial \zeta\left[z(t_k) \mid z^{k-1};\alpha\right]}{\partial\alpha_i} + \frac{\partial \zeta[x(t_0);\alpha]}{\partial\alpha_i} \tag{12}$$

where [for the trace term see Eq. (25)]

$$\frac{\partial \zeta\left[z(t_k) \mid z^{k-1};\alpha\right]}{\partial\alpha_i} = \frac{1}{2}\mathrm{trace}\left[S(t_k)^{-1}\frac{\partial S(t_k)}{\partial\alpha_i}\right] + r(t_k)^T \times S(t_k)^{-1}\frac{\partial r(t_k)}{\partial\alpha_i} - \frac{1}{2} r(t_k)^T S(t_k)^{-1}\frac{\partial S(t_k)}{\partial\alpha_i} S(t_k)^{-1} r(t_k) \tag{13}$$

$$\frac{\partial \zeta[x(t_0);\alpha]}{\partial\alpha_i} = \frac{1}{2}\mathrm{trace}\left[P_0^{-1}\frac{\partial P_0}{\partial\alpha_i}\right] \tag{14}$$

The Fisher information approximation to the coefficient matrix in Eq. (1) is[10,12]

$$A_{ij} \approx \mathbb{I}_{ij} = \sum_{k=1}^{N}\left\{\mathrm{trace}\left[\frac{\partial r(t_k)^T}{\partial\alpha_i}\frac{\partial r(t_k)}{\partial\alpha_j} S(t_k)^{-1}\right] + \frac{1}{2}\mathrm{trace}\left[\frac{\partial S(t_k)}{\partial\alpha_i} S(t_k)^{-1}\frac{\partial S(t_k)}{\partial\alpha_j} S(t_k)^{-1}\right]\right\} + \mathrm{trace}\left[\frac{\partial x_0^T}{\partial\alpha_i}\frac{\partial x_0}{\partial\alpha_j} P_0^{-1}\right] + \frac{1}{2}\mathrm{trace}\left[\frac{\partial P_0}{\partial\alpha_i} P_0^{-1}\frac{\partial P_0}{\partial\alpha_j} P_0^{-1}\right] \tag{15}$$

IV. System Identification Results

We model trend, random walk, exponentially correlated, and white noise by Eqs. (4) and (5) with $\Delta t = t_k - t_{k-1}$, $H = [1\ 1]$, $R = [v^2]$, $Bu = [a\Delta t\ 0]^T$, and

$$\Phi = \begin{bmatrix} 1 & 0 \\ 0 & e^{-c_1\Delta t} \end{bmatrix}, \qquad L = \begin{bmatrix} b & 0 \\ 0 & c_1 c_2 \end{bmatrix}$$

$$Q = \Delta t\begin{bmatrix} 1 & 0 \\ 0 & 1 \end{bmatrix} \tag{16}$$

The system identification estimates from fitting to simulated data with random number generated Wiener process Gaussian increments $\xi_i(t_k)$ every $\Delta t = 0.1$ s are given in Table 1. The first two result columns solve for all parameters except uncorrelated initial state standard deviations, which were assumed to be 0.01 and 0.1, respectively. The last column gives the estimates for a one-state model without exponentially correlated noise.

Estimates of trend, random walk, and white noise parameters are insensitive to the values of the initial state standard deviations. More frequent data are required to estimate the exponentially correlated noise parameters and obtain a positive scaling parameter.

The PSD calculated from real 1-s input-axis-vertical accelerometer data is the solid line in Fig. 1 with a high-frequency +2 log-log quantization line slope and an approximately −1 log-log low-frequency slope. The PSD of 10-s averaged data is the dotted line in Fig. 1.

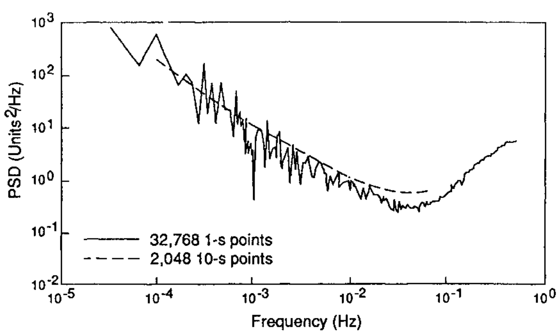

Fig. 1 Power spectral density of input-axis-vertical accelerometer output.

Table 1 Results of system identification fits to simulated sample paths (trend, random walk, exponentially correlated, and white noise for 3276 0.1-s points)

Parameter	True values	Estimated values $P_0 = 0.01^2$	$P_0 = 0.1^2$	$P_0 = 0.1^2$
Initial cond.: x_1, units	0.00	0.0006 ± 0.01	0.058 ± 0.01	-0.045 ± 0.096
x_2, units	0.00	-0.0002 ± 0.01	-0.013 ± 0.1	——
Trend: a, units/s	1.00	0.982 ± 0.054	0.982 ± 0.054	0.982 ± 0.054
Random walk st. dev b	1.00	0.988 ± 0.10	0.987 ± 0.10	0.981 ± 0.023
Exp. corr. noise:				not included
Inv. time const. c_1, $1/s$	0.64	1.843 ± 0.40	1.842 ± 0.40	0.00
Scaling param. c_2, units	1.56	-0.869 ± 0.23	-0.870 ± 0.23	0.00
White noise st. dev. v, units	0.10	0.160 ± 0.031	0.160 ± 0.031	0.142 ± 0.008

Table 2 Results of system identification fit to 10-s averaged accelerometer data (initial state standard deviations 10, 1)

Parameter	3000 points	4850 points
Initial cond.: x_1, units	0.00 ± 10.0	0.10 ± 10.0
x_2, units	-0.158 ± 1.0	0.002 ± 1.0
Trend: a, units/s	$2.09 \times 10^{-5} \pm 2.8 \times 10^{-5}$	$7.94 \times 10^{-7} \pm 2.7 \times 10^{-5}$
Random walk st. dev. b	$5.10 \times 10^{-3} \pm 1.2 \times 10^{-3}$	$5.89 \times 10^{-3} \pm 1.0 \times 10^{-3}$
Exp. corr. noise:		
Inv. time const. c_1, 1/s	$5.74 \times 10^{-3} \pm 1.5 \times 10^{-3}$	$6.59 \times 10^{-3} \pm 1.4 \times 10^{-3}$
Scaling param. c_2, units	2.70 ± 0.86	2.76 ± 0.54
White noise st. dev. v, units	0.174 ± 0.003	0.173 ± 0.002
Rms pre-update residual, units	0.20	0.20

The results of fitting model Eqs. (4), (5), and (16) to 3000 and 4850 points of 10-s averaged accelerometer data are given in Table 2. The PSD of a simulated sample path using the estimated parameters was almost the same as the dotted line in Fig. 1, showing that flicker noise has been approximated by a combination of random walk, exponentially correlated, and white noise.

V. Fractional Brownian Motion Parameter Estimation

Fractional Brownian motion $\beta_H(0 < H < 1)$ is defined as a mean-square-continuous zero-mean Gaussian stochastic process by the Ito stochastic integral[4,5]:

$$\beta_H(t,\omega) = \frac{1}{\Gamma(H+0.5)} \times \left\{ \int_{-\infty}^{0} \left[(t-s)^{H-1/2} - (-s)^{H-1/2}\right] \mathrm{d}\beta(s,\omega) + \int_0^t (t-s)^{H-1/2}\, \mathrm{d}\beta(s,\omega) \right\} \tag{17}$$

where ω is the probability variable and β is a Wiener random walk process. The log-log PSD slope of fBm is $-(1+2H)$.

The non-Markov fBm has stationary, self-similar, but not independent increments (except when $H = 0.5$ for ordinary Brownian motion) with covariance[4]

$$E\left\{[\beta_H(t+\tau) - \beta_H(t)]^2\right\} = V_H \tau^{2H} \qquad (V_H = \text{const}) \tag{18}$$

Let β_H now denote a constant times fBm. Its autocorrelation at times $t_j = j\Delta t$ and $t_k = k\Delta t$ is[6,12]

$$\phi_{\beta\beta}(j,k) = E\{\beta_H(t_j)\beta_H(t_k)\} = \tfrac{1}{2}\sigma_H^2 \Delta t^{2H}[|j|^{2H} + |k|^{2H} - |j-k|^{2H}] \tag{19}$$

where $\sigma_H = V_H$ times the constant. The correlation or covariance between two zero-mean fBm increments $X(t_k) = \beta_H(t_{k+1}) - \beta_H(t_k)$ is[6,12]

$$\phi_{xx}(k+n,k) = E\{X(t_{k+n})X(t_k)\} = \tfrac{1}{2}\Delta t^{2H}\sigma_H^2[|n+1|^{2H} - 2|n|^{2H} + |n-1|^{2H}] \tag{20}$$

so that $\phi_{xx}(k+n,k) = \phi_{xx}(n)$.

If measurements z_k are fBm (or fBm increments) plus a bias b, then the joint probability density of the measurements is

$$p(z_1,\ldots,z_N) = (2\pi)^{-N/2}\det(S)^{-1/2} e^{-(z-b)^T S^{-1}(z-b)/2} \tag{21}$$

$$S_{ij} = \begin{cases} \phi_{\beta\beta}(i,j) & \text{fBm} \\ \phi_{xx}(|i-j|) & \text{fBm increments} \end{cases} \tag{22}$$

If there is a trend in the data in addition to noise, then $b = a_0 + a_1 k\Delta t$ for the fBm case, and $b = a_1\Delta t$ for the fBm increment case.

If white noise with standard deviation σ_m and exponentially correlated noise with reciprocal time constant c_1 and scaling parameter c_2 are additive to and uncorrelated with the fBm noise in the measurements, then[12]

$$S_{ij} = \phi_{\beta\beta}(i,j) + \sigma_m\delta_{ij} + \frac{c_1c_2^2}{2} e^{-c_1|i-j|\Delta t} \tag{23}$$

In the fBm increment case,[12]

$$S_{ij} = \phi_{xx}(|i-j|) + \sigma_m(2\delta_{|i-j|,0} - \delta_{|i-j|,1}) + \frac{c_1c_2^2}{2}[2e^{-c_1|i-j|\Delta t} - e^{-c_1|i-j-1|\Delta t} - e^{-c_1|i-j+1|\Delta t}] \tag{24}$$

The partial derivatives of the negative log likelihood with respect to the noise and trend parameters are straightforward to calculate from Eqs. (21–24) using[12]

$$\frac{\partial \ln[\det(S)]}{\partial\alpha} = \operatorname{trace}\left[S^{-1}\frac{\partial S}{\partial\alpha}\right] \tag{25}$$

VI. Fractional Brownian Estimation Results

Iterative maximum likelihood fits were done to 128 simulated[6] fBm data points with the fBm and fBm increment models with $\Delta t = 1.0$ s. Both techniques yielded the same results close to the true values $H = 0.1$ and $\sigma_H = 1.0$:

$$H = 0.109 \pm 0.03, \qquad \sigma_H = 0.988 \pm 0.07 \tag{26}$$

Table 3 Parameter estimates from fits to simulated fBm plus trend (σ_H = 0.7, H = 0.4, Δt = 1.0 s, 128 points)

Case	a	σ_H	H
1) $a = 1.5$	1.486 ± 0.02	0.914 ± 0.04	0.301 ± 0.03
2) $a = 5.0$	4.986 ± 0.02	0.914 ± 0.04	0.301 ± 0.03

Table 4 Parameter estimates from fits to simulated fBm plus white noise (σ_H = 0.7, H = 0.4, Δt = 1.0 s)

Case	σ_m	σ_H	H
1) $\sigma_m = 0.025$ (128 pts)	0.271 ± 0.09	0.522 ± 0.09	0.599 ± 0.11
2) $\sigma_m = 0.25$ (128 pts)	0.353 ± 0.16	0.651 ± 0.17	0.461 ± 0.13
3) $\sigma_m = 0.25$ (200 pts)	0.402 ± 0.08	0.571 ± 0.10	0.556 ± 0.10
4) $\sigma_m = 1.00$ (128 pts)	——	——	——
5) $\sigma_m = 1.00$ (200 pts)	0.838 ± 0.19	0.899 ± 0.32	0.350 ± 0.13

The results of fitting to simulated fBm plus a trend and to simulated fBm plus white noise with the increment model are given in Tables 3 and 4. Case 4 in Table 4 would not converge until the number of data points was raised from $n = 128$ to 200 in case 5.

Fits to simulated fBm plus exponentially correlated noise with $\Delta t = 1.0$, $H = 0.4$, $\sigma_H = 0.7$, $c_1 = 0.5$, and $c_2 = 0.9$ failed with $n = 128$ and 200 measurements.

Fractional Brownian motion parameters were estimated from 128 points of 150-s averaged accelerometer data from Fig. 1:

$$H = 0.212 \pm 0.04, \qquad \sigma_H = 2.725 \pm 0.72 \tag{27}$$

which yields a log-log PSD slope of -1.424.

References

[1]Hooge, F., "Discussion of Recent Experiments in $1/f$ Noise," *Physica*, Vol. 60, 1972, pp. 130–144.

[2]Solo, V., "Intrinsic Random Functions and the Paradox of $1/f$ Noise," *SIAM Journal on Applied Mathematics*, Vol. 52, 1992, pp. 270–291.

[3]Keshner, M., "$1/f$ Noise," *Proceedings of the Institute of Electrical and Electronics Engineers*, Vol. 70, 1982, pp. 212–218.

[4]Mandlebrot, B., and Van Ness, J., "Fractional Brownian Motions, Fractional Noises and Applications," *Society for Industrial and Applied Mathematics Review*, Vol. 10, 1969, pp. 422–437.

[5]Flandrin, P., "On the Spectrum of Fractional Brownian Motions," *IEEE Transactions on Information Theory*, Vol. 35, 1989, pp. 197–199.

[6]Lundahl, T., Ohley, W., Kay, S., and Siffert, R., "Fractional Brownian Motion: A Maximum Likelihood Estimator and Its Application to Image Texture," *IEEE Transactions on Medical Imaging*, Vol. MI-5, 1986, pp. 152–161.

[7]Maybeck, P., *Stochastic Models, Estimation, and Control*, Vol. 2, Academic, San Diego, CA, 1982, Chap. 10.

[8]Maybeck, P., "Combined State and Parameter Estimation for On-Line Applications," Ph.D. Dissertation, Massachusetts Inst. of Technology, Cambridge, MA, Feb. 1972.

[9]Gupta, N., and Mehra, R., "Computational Aspects of Maximum Likelihood Estimation and Reduction in Sensitivity Function Calculations," *IEEE Transactions on Automatic Control*, Vol. AC-19, 1974, pp. 774–783.

[10]Sandell, N., Jr., and Yared, K., "Maximum Likelihood Identification of State Space Models for Linear Dynamic Systems," Massachusetts Inst. of Technology Electronic Systems Lab., Rep. ESL-R-814, Cambridge, MA, 1978.

[11]Taylor, R., "Dynamic System Identification Based on Propagation of Probability Densities and Their Partial Derivatives," Draper Lab., Rept. CSDL-P-1929, Cambridge, MA, 1984.

[12]Skeen, M., "Maximum Likelihood Estimation of Fractional Brownian Motion and Markov Noise Parameters," M.S. Thesis, Massachusetts Inst. of Technology, Cambridge, MA, 1992.

Aircraft Controller Synthesis by Solving a Nonconvex Optimization Problem

R. Srichander*

Technische Universität Berlin, 10587 Berlin, Germany

Introduction

A DESIGN technique for the synthesis of the pitch axis controller for an aircraft is presented in this Note. The proposed technique assumes a single-input multi-output system, and the type and order of the controller are assumed to be selected by the designer to reflect specific design requirements. The controller design problem is posed as a parameter optimization problem where the objective function is to minimize the infinity norm of a suitable error transfer function.

Formulation of the controller design problem as a parameter optimization problem with a time-domain performance criterion has been examined earlier,[1,2] and the problem has been solved using nonlinear programming (NLP) techniques. Unfortunately, the parameter optimization problem for fixed-order compensators is invariably nonconvex in the space of the design parameters, and hence, only a local minimum can be obtained. Direct design of low-order compensators using other techniques also leads to solutions having many local minima.[3]

In this Note, the controller design problem is formulated as a frequency-domain model-matching problem. The proposed technique is new both in the way the optimization problem is formulated and in the solution method used to find the optimal design parameters. In particular, we use the simulated annealing (SA) technique[4,5] to solve the optimization problem since this problem is nonconvex in the space of the design parameters. The application of the SA technique to solve controller design problems is new, and this Note explores the applicability of SA to controller design problems by considering a practical example from the field of aircraft control. For the sake of comparison, the solution to the optimization problem obtained using the NLP technique is also presented.

Problem Formulation

The specific problem to be considered here is the design of the pitch axis controller of an aircraft. It is assumed that the linearized longitudinal dynamics of the aircraft can be represented by the state-space description

$$\dot{x} = Ax + B\delta_e \qquad y = Cx + D\delta_e \tag{1}$$

where δ_e is the elevator input. The state-variable matrices for the design example considered are given in Table 1. Here it is assumed that the output variables available for feedback are pitch rate q, normal acceleration nz, and angle of attack α. For the purpose of illustrating the design technique, it is assumed that the controller structure to be implemented in the various loops have the form shown in Fig.1. In practice, the controller type and order can be completely arbitrary in each of the loops and, further, the number of feedback loops are also not fixed a priori. The only point to be kept in mind is that, given a single input, it is possible to arbitrarily shape only one output variable of interest.

Again for the purpose of illustration, it is assumed that the pitch rate is the output variable of interest, whose response has to be shaped to meet the handling quality specifications.[6] In particular, MIL-STD-1797A[6] requires that, for flight phases other than landing and take-off (which include air-to-air combat, rapid maneuvering,

Received Aug. 30, 1993, revision received Dec. 23, 1993; accepted for publication March 7, 1994.

*Guest Scientist; currently Financial Engineer, Ehd 1, Credit Suisse, CH-8070 Zurich, Switzerland.